HEATH, G. A., MASON, R. & THOMAS, K. M. (1974). *J. Amer. Chem. Soc.* **96**, 259–260.
IBRAHIM, E. H. M., SHAW, R. A., SMITH, B. C., THAKUR, C. P., WOODS, M., BULLEN, G. J., RUTHERFORD, J. S., TUCKER, P. A., CAMERON, T. S., HOWLETT, K. D. & PROUT, C. K. (1971). *Phosphorus*, **1**, 153–155.
International Tables for X-ray Crystallography (1962). Bd. III, S. 213. Birmingham: Kynoch Press.
JOHNSON, C. K. (1965). Oak Ridge National Laboratory. Report ORNL 3794, Revised.
JÜRGENS, G. (1973). Diplomarbeit, Freie Universität Berlin.
KRONBERG, W. L. & HARKER, D. (1942). *J. Chem. Phys.* **10**, 309–317.
MITCHELL, K. A. R. (1969). *Chem. Rev.* **69**, 157–178.
NITTA, I., SAKURAI, K. & TOMIIE, Y. (1951). *Acta Cryst.* **4**, 289–293.
OLTHOF, R., MIGCHELSEN, T. & VOS, A. (1965*a*). *Acta Cryst.* **19**, 596–603.
OLTHOF, R., MIGCHELSEN, T. & VOS, A. (1965*b*). *Acta Cryst.* **19**, 603–610.
PAULING, L. (1960). *The Nature of the Chemical Bond*, 3. Aufl. Ithaca: Cornell Univ. Press.
PETERSON, M. B. & WAGNER, A. J. (1973). *J. Chem. Soc. Dalton*, S. 106–111.
SAKURAI, K. & TOMIIE, Y. (1952). *Acta Cryst.* **5**, 293–294.
SCHOMAKER, V. & STEVENSON, D. P. (1941). *J. Amer. Chem. Soc.* **63**, 37–40.
STEWART, J. M. (1972). The X-RAY System, version of June 1972. Technical Report TR 192, Computer Science Center, Univ. of Maryland.
TOLKMITH, H. & BRITTON, E. C. (1959). *J. Org. Chem.* **24**, 705–708.
WEISS, J. & HARTMANN, C. (1966). *Z. Naturforsch.* **21b**, 891–892.
YAMAGUCHI, A., ICHISHIMA, I., SHIMANOUCHI, T. & MIZUSHIMA, S. (1959). *J. Chem. Phys.* **31**, 843.

Acta Cryst. (1975). B**31**, 2105

Haycockite, $Cu_4Fe_5S_8$: a Superstructure in the Chalcopyrite Series

BY J. F. ROWLAND AND S. R. HALL

Mineral Science Laboratories, CANMET, Department of Energy, Mines and Resources, 555 Booth Street, Ottawa, Canada, K1A 0G1

(*Received* 18 *November* 1974; *accepted* 24 *February* 1975)

Haycockite, $Cu_4Fe_5S_8$, is a mineral closely related to chalcopyrite $CuFeS_2$, talnakhite, $Cu_9Fe_8S_{16}$ and mooihoekite $Cu_9Fe_9S_{16}$. A single crystal of haycockite from the Lydenburg District, Transvaal, South Africa was studied with three-dimensional X-ray diffraction techniques. The crystal cell is orthorhombic, $a = 10{\cdot}705$ (5), $b = 10{\cdot}734$ (5), $c = 31{\cdot}630$ (15) Å with the possible space groups $P222$, $P222_1$, $P2_12_12$, $P2_12_12_1$. Haycockite exhibits a strong tendency to twin in the plane (103). This twinning, and the superlattice nature of the structure, restricted the measurement of diffraction data and limited structural resolution of the analysis. The atomic arrangement was determined primarily in terms of the subcell ordering.

Introduction

Haycockite was identified as a distinct mineral, closely related to chalcopyrite $CuFeS_2$, by Cabri & Hall (1972). Previous structural studies of talnakhite $Cu_8Fe_9S_{16}$ (Hall & Gabe, 1972) and mooihoekite $Cu_9Fe_9S_{16}$ (Hall & Rowland, 1973) showed these minerals to have a similar chalcopyrite-like arrangement of metals and sulphurs, but to differ in the ordering of interstitial metal atoms. From the outset, the structural study of haycockite represented a considerably more difficult problem than that posed by either talnakhite or mooihoekite. First, haycockite has been found only as fine-grained lamellae and most are microcrystalline (Cabri & Hall, 1972). In contrast to mooihoekite, however, it has not been possible to synthesize haycockite (Cabri, 1973). Second, all the haycockite fragments examined exhibited substantial integral-twinning and this severely complicates data collection. Third, the intensity data of haycockite are dominated by two subcells, the smaller being a sphalerite-like pseudo-cubic subcell ($a \simeq 5{\cdot}3$ Å), and the larger a pseudo-tetragonal subcell ($a \simeq 5{\cdot}3$, $c \simeq 16$ Å). These subcells, coupled with the small crystal size, result in an extremely high proportion of very weak reflexions. Another problem associated with the superlattice nature of the haycockite structure was the uncertainty of the systematic absences in diffraction data used to identify the space-group symmetry. And last, the large number of independent atomic sites in the haycockite cell posed severe computational constraints in the refinement of these parameters which, coupled with a low data-to-parameter ratio, diminishes the validity of the least-squares process.

The conclusions drawn from this investigation, therefore, must be made in the light of all these factors.

Even so, we believe that the general structural features are established by this study, and that these are both consistent with those found in the related minerals, and sufficient to distinguish haycockite as a structurally distinct entity.

Experimental

Crystal data

Source: Natural material from Lydenburg District, Transvaal, South Africa. Microprobe analysis (wt.%): Cu: 32·2 (4), Fe: 35·0 (5), Ni: 0·4 (2), S: 32·4 (5). Chemical composition: $Cu_{1\cdot00}(Fe_{1\cdot24}Ni_{0\cdot01})S_{2\cdot00}$. Stoichiometric formula: $Cu_4Fe_5S_8$. Possible systematic hkl absences: $h00$ $h=2n+1$, $0k0$ $k=2n+1$, $00l$ $l=2n+1$. Possible space groups: $P222$ (No. 16), $P222_1$ (No. 17), $P2_12_12$ (No. 18) or $P2_12_12_1$ (No. 19). Cell dimensions: $a=10\cdot705$ (5), $b=10\cdot734$ (5), $c=31\cdot630$ (15) Å, $Z=12$, $D_{calc}=4\cdot33$ g cm^{-3}. Linear absorption coefficient: μ(Mo $K\alpha$) = 140 cm^{-1}. Intensity data: 2890 reflexions measured.

Owing to the microcrystalline nature of the haycockite specimens, only one grain was found that was of suitable size for single-crystal X-ray diffraction analysis. The haycockite grain approximated to an irregular tetrahedron in shape, with four large and three small faces, and with the largest dimension about 0·25 mm. Because of the unavailability of other material, no attempt was made to grind a sphere.

A survey of the diffraction data from precession camera films clearly showed the presence of two predominant subcells. The superlattice nature of the data was subsequently confirmed with the four-circle diffractometer. The most intense reflexions can be indexed on a pseudo-cubic face-centred cell ($a\simeq5\cdot3$ Å), and additional strong reflexions can be indexed on a pseudo-tetragonal subcell with dimensions $a=5\cdot352$, $b=5\cdot367$, $c=15\cdot815$ Å. To index all reflexions, an orthorhombic cell with dimensions $a=10\cdot705$, $b=10\cdot734$, $c=31\cdot630$ Å is required. For this cell, all the strong reflexions satisfy the condition $h,k,l=2n$, while most of the additional weak reflexions satisfy the condition $h,k,l=2n+1$. The cell is not face-centred, however, because there are many weak reflexions that violate the systematic absence condition $h+k,k+l,(l+h)=2n$. Although the reflexions along the cell axes conform to the systematic-absence conditions $h00$: $h=2n$, $0k0$: $k=2n$, $00l$: $l=2n$, this may actually result from the dominant symmetry of the sublattice, rather than truly represent the space-group conditions of the unit cell. Assuming that the pseudo-cubic subcell implies a tetrahedral arrangement of atoms, as is the case for all other chalcopyrite-like structures, the possible space groups are $P222$, $P222_1$, $P2_12_12$ or $P2_12_12_1$.

The precession camera films also showed the presence of three twin-components, two of approximately equal volume and a third that was much smaller. The first two components had coincident b axes and the approximate directions of the a and c axes interchanged, while the first and third components had coincident a axes and the approximate directions of the b and c axes interchanged. The twinning occurs along the (103) planes (see Fig. 1).

Alignment of suitable reflexions on an automatic four-circle diffractometer permitted the determination of the orientation matrix and the calculation of the cell parameters for the first of the two strong twin-components. The reflexions were chosen carefully in order to avoid those significantly affected by twinning. This choice was severely limited by the fact that all reflexions were broad, and those with sufficient intensity for the alignment process were generally subject to twinning. The angles 2θ, χ and ω were obtained from an automatic alignment process (Busing, 1970) with the four equivalents of each of the reflexions 840, 480, 8,0,12, 0,8,12, 4,0,24 and 0,4,24. The refined unit-cell values were $a=10\cdot705$ (5), $b=10\cdot734$ (5), $c=31\cdot630$ (15) Å, and $\alpha=\beta=\gamma=90\cdot00$ (2)°. The orientation matrix was similarly determined for the other large

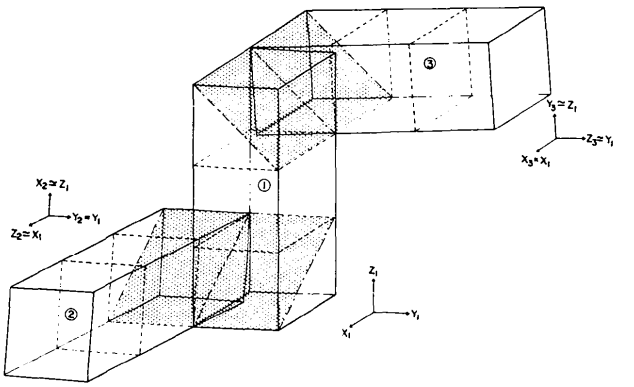

Fig. 1. Twinning in haycockite. Twin planes are stippled.

Table 1. *Reflexion data*

Number of reflexions with $I_{net}>1\cdot65\sigma(I)$ in brackets. Number of reflexions not measured in italics.

	Number of reflexions for each 2θ range				
h,k,l conditions	0–29°	29–41°	41–81°	81–97°	Total
$h,k=2n$, $l=6n$ only	49 (48)	65 (52)	487 (176)	305 (85)	906 (361)
Additional data with $h,k,l=2n$	78 (50)	125 (61)	926 (219)	*582*	1129 (330)
Additional data with $h+k,k+l,(l+h)=2n$	82 (21)	151 (21)	*1234*	*776*	233 (42)
Additional data with no conditions	622 (68)	*981*	*8000*	*4982*	622 (68)
Reflexions collected	831 (187)	341 (134)	1413 (395)	305 (85)	2890 (801)

twin-component, but with less accuracy, and the unit-cell dimensions were within the e.s.d.'s of the values given above. The difference in the calculated **a** and **b** dimensions is very small (*ca.* 0·3 %) but significant. The non-equivalence of a and b is consistent with the differences in intensities of $h0l$ and $0kl$ reflexions.

The relative proportions of the three twin-components, estimated from the intensities of the 24 reflexions used in the orientation-matrix calculation are 1·00: 0·90 (5): 0·10 (3). The twin-components are related as follows: Twin No. 1 to twin No. 2 (twin plane {103}) $b_1=b_2$, $[h00]_1\simeq[00l]_2$, $[00l]_1\simeq[h00]_2$. Twin No. 1 to twin No. 3 (twin plane {013}) $a_1=a_3$, $[0k0]_1\simeq[00l]_3$, $[00l]_1\simeq[0k0]_3$.

The intensity data used in this analysis were collected on the first twin-component. Any contribution to intensities by the second twin-component was appropriately subtracted. This was required for only intense reflexions with $h=2n$, $k=2n$ and $l=6n$. Contributions by the third twin-component were not considered significant.

All intensity data for haycockite were measured on an automatic four-circle diffractometer using graphite-monochromated Mo $K\alpha$ radiation. The $\theta/2\theta$ scan width (3·0 to 3·8°) was adjusted automatically for α_1–α_2 dispersion, and the background counts were measured on each side of the peak for approximately the same length of time as that required for the scan. The intensities of three reference reflexions were recorded after every 50 measurements in order to monitor the crystal alignment and instrument stability. No significant variations were noted during the data collection.

Because of the superstructure nature of haycockite, most of the intensity data in the Mo $K\alpha$ Ewald sphere are extremely weak. It was impractical, therefore, to measure all unique data, and a variable data-collection scheme, that involved different 2θ and h,k,l constraints, was used to examine only those areas of reciprocal space where significant intensities were expected. Table 1 shows that the proportion of intensities with $I_{net}>1{\cdot}65\ \sigma(I)$ is dependent on the h,k,l conditions, due to the various subcells, and decreases with increasing 2θ. The 2θ values beyond which the h,k,l constraints were introduced were carefully chosen so that the proportions of significant intensities were negligible. For instance, beyond $2\theta=29°$ no significant data were expected with the condition $h+k,k+l,(l+h)=2n+1$. Using this approach, 2890 reflexions were measured in one octant of the first twin-component, and 801 had net intensities with $I_{net}>1{\cdot}65\sigma(I)$, and 16555 additional reflexions were not examined. Reflexions with net intensities below this level were set a threshold intensity of $1{\cdot}65\sigma(I)$ and coded as 'less thans' for the purposes of refinement.

Corrections to the net intensities were made for overlap of the second twin-component taking into consideration the relative orientations of the twin-components at specific φ, χ and low 2θ values. The 'detwinned' intensities were then adjusted for absorption effects, with a generalized Gaussian procedure (Gabe & O'Byrne, 1970), and reduced to structure factors by application of Lorentz and polarization factors.

Structure determination

Structure indicators

As described earlier, the intense reflexions in the diffraction data clearly establish the superstructure nature of haycockite. The first level of substructure is based on the small pseudo-cubic subcell ($a\simeq5{\cdot}3$ Å) similar to that in talnakhite (Hall & Gabe, 1972) and mooihoekite (Hall & Rowland, 1973), and is consistent with a structure based on a sphalerite-like arrangement of metal and sulphur atoms.

The second level of substructure is based on the pseudo-tetragonal subcell ($a\simeq5{\cdot}3$, $c\simeq16$ Å), and it was expected that this pertained in large part to the arrangement of the metal atoms that are in addition to those in the sphalerite-like arrangement. The additional metal atoms have been shown to be in interstitial sites in talnakhite and mooihoekite and, because haycockite is also metal-rich, a similar arrangement was expected in this structure.

Additional structural information was deduced from the relative size of the cell dimensions. When reduced to a pseudo-cubic cell, the cell lengths are 5·352, 5·367, and 5·272 Å, along the a, b and c directions, respectively. In mooihoekite, expansion of the pseudo-cubic cell beyond 5·29 Å occurs only when additional metal atoms occupy all the interstitial sites along an axis. Under these circumstances the displacement of adjacent metal atoms by the interstitial atoms cannot take place without a significant cell expansion. In mooihoekite this results in a c dimension of 5·383 Å. On the other hand, when the additional metal atoms occupy only alternate interstitial sites along an axis, the resulting metal shifts can be taken up within the structure without a substantial cell change in this direction. This is the case for all axes in talnakhite, and for the a and b axes in mooihoekite. One may deduce, therefore, from the relative size of the haycockite axes, that in parts of the structure adjacent interstitial metal sites are occupied along the **a** and **b** directions, but not along the **c** direction.

These three indicators, the pseudo-cubic subcell, the pseudo-tetragonal subcell, and the relative size of the cell dimensions, were the basis for the structural solution of haycockite.

Pseudo-cubic subcell

The pseudo-cubic subcell with $a\simeq5{\cdot}3$ Å was assumed to contain a sphalerite-like arrangement of metal and sulphur atoms as in other chalcopyrite-like minerals. The atoms were located in tetrahedrally coordinated sites of space group $F\bar{4}3m$, with the metal atoms at 4(a) (0,0,0) and the sulphur atoms at 4(d) $(\frac{3}{4},\frac{3}{4},\frac{3}{4})$. No structure work was done with the pseudo-cubic subcell directly, but an initial structure-factor

calculation (see below) was based solely on the sphalerite-like arrangement of atoms.

Pseudo-tetragonal subcell

The sphalerite-like arrangement of atoms was transformed into the pseudo-tetragonal subcell by combining three pseudo-cubic cells along the **c** direction. The space group used for this subcell was orthorhombic $P222$, one of the possible space groups for the true unit cell. The ideal sites in the pseudo-tetragonal cell for the 12 metal atoms are at 1(*b*) $(\frac{1}{2},0,0)$, 1(*c*) $(0,\frac{1}{2},0)$, 1(*d*) $(0,0,\frac{1}{2})$, 1(*h*) $(\frac{1}{2},\frac{1}{2},\frac{1}{2})$, 2(*q*) $(0,0,\frac{1}{6})$, 2(*r*) $(\frac{1}{2},0,\frac{1}{3})$, 2(*s*) $(0,\frac{1}{2},\frac{1}{3})$ and 2(*t*) $(\frac{1}{2},\frac{1}{2},\frac{1}{6})$, and for the 12 sulphur atoms at 4(*u*) $(\frac{1}{4},\frac{1}{4},\frac{1}{12})$, 4(*u*) $(\frac{1}{4},\frac{3}{4},\frac{1}{4})$ and 4(*u*) $(\frac{1}{4},\frac{1}{4},\frac{5}{12})$. The intensity data set for the large orthorhombic cell was modified to include only reflexions with $h,k,l=2n$, and these indices were divided by two. The resulting data set contained 2035 reflexions of which 689 had net intensities with $I_{net} > 1{\cdot}65\sigma(I)$.

In these calculations, the Hartree–Fock scattering factors of Cromer & Mann (1968) for neutral atoms were used, with the values for copper and iron combined in proportion to the composition to give the metal scattering factors. These, and all subsequent calculations, were done on a CDC 6400 computer with the X-RAY system of crystallographic programs (Stewart *et al.*, 1972).

In the initial structure-factor calculation the metal and sulphur atoms were placed in the ideal sites listed above, corresponding to the sphalerite-like arrangement of the pseudo-cubic subcell, and isotropic temperature factors of 1·0 Å were used. The R value $(\sum|\Delta F|/\sum|F_o|)$ was 0·61 ('less thans' omitted). A subsequent electron-density difference map showed 12 large positive maxima corresponding to the possible locations of the interstitial metal atoms. However, the difference map did not indicate significant shifts of the input atoms, and this made the location of the extra metal atoms difficult. In the first instance, an extra metal atom was arbitrarily placed at 1(*a*) (0,0,0) and this resulted in a decrease in the R value to 0·35. The electron-density difference map showed positive maxima as before, except for $z=0$, where negative maxima occurred. Substantial shifts of both metal and sulphur atoms were indicated along the c axis away from $z=0$. Small random shifts not related to the extra metal site were indicated for the sulphur atoms along the a and b axes.

Relative cell lengths

When the atoms were shifted in the directions indicated in the difference map, the R value decreased to 0·28. This reduced substantially the residuals occurring at $z \simeq \pm\frac{1}{6}$ and $z \simeq \pm\frac{1}{3}$, but not those at $z=\frac{1}{2}$. Locating an additional metal atom at $z=\frac{1}{2}$ is consistent with the $c:a$ ratio being about 3:1, because extra metal atoms occupy adjacent interstitial sites along the a and b axes, but only every third interstitial site along the c axis. These locations of extra metal atoms would give parameter shifts along the c axis and lattice expansion along the a and b axes, consistent with the relative dimensions of the pseudo-cubic subcell. Continuing in this manner, that is, shifting atoms as indicated by the electron-density map, and placing the $1\frac{1}{2}$ extra metal atoms with appropriate fractional population parameters in various sites with $z=0$ and $\frac{1}{2}$, the structure-factor calculations resulted in a decrease in the R value to only about 0·21.

Various isotropic temperature factors were introduced, and scattering factors for ionized atoms were used, those of Cromer & Mann (1968) for copper and iron, and those of Tomiie & Stam (1958) for sulphur. The lowest R value obtained was about 0·18, with the extra atoms located at 1(*a*) (0,0,0) with a population parameter (p.p.) of 1 and at 1(*f*) $(\frac{1}{2},0,\frac{1}{2})$ with p.p. of $\frac{1}{2}$. Significant distorted negative maxima occurred at atom locations, and significant positive or negative maxima occurred at the interstitial sites. Effects attributed to anisotropy were noted, but the introduction of anisotropic temperature factors made little difference. No attempt was made to distinguish between copper and iron atoms at this time, and it was concluded that the limit had been reached in the usefulness of the pseudo-tetragonal cell as a basis for structure analysis.

Orthorhombic cell

There were only 112 reflexions with $I_{net} > 1{\cdot}65\sigma(I)$ that required the large orthorhombic unit cell with $a=10{\cdot}705$, $b=10{\cdot}734$ and $c=31{\cdot}630$ Å, and all had weak intensities. These reflexions, however, are considered critical in determining the locations of the extra metal atoms.

The atomic coordinates for the orthorhombic cell were derived from those obtained for the pseudo-tetragonal subcell. In this derivation the same idealized sphalerite-like sites are obtained for each of the four possible orthorhombic space groups, $P222$, $P222_1$, $P2_12_12$ and $P2_12_12_1$, although there are different site equivalences. For each of these space groups, 96 sulphur atoms are located in 24 general positions. In space group $P2_12_12_1$, the 96 metal atoms are located in 24 general positions, while in the other three space groups some of the metal atoms occur in special positions. In space group $P222$, 56 metal atoms are located in 14 general positions and the rest in 20 special positions.

The sites for the extra metal atoms in the orthorhombic cell were similarly derived from those for the pseudo-tetragonal subcell. These sites occur in planes along the c axis, with four atoms at $z=0$ and at $z=\frac{1}{2}$, and four half-atoms at $z \simeq 0{\cdot}25$ and $z \simeq 0{\cdot}75$. The equivalences of these sites depend on the space group used, with $P222$ having more extra metal atoms in special positions.

Structure factors were calculated using these orthorhombic atomic sites for both the space groups $P222$ and $P2_12_12_1$, and the R value was about 0·31 in each case. The difference maps showed residuals that were

attributable to both substantial atomic shifts along all three axes for most atoms, and to the location of the additional metals in certain of the interstitial sites. Several rounds of structure-factor and difference-map calculations provided shifts to the atomic parameters and temperature factors, and also a re-distribution of the extra metal atoms into specific sites. The new locations were equivalent to an origin shift of $x=\frac{1}{4}$, $z=\frac{1}{4}$, and these sites can be expressed in space group $P222$ without requiring partial occupancy.

Although the difference map showed significant residuals, further refinement did not reduce the R value below 0·22. It was apparent that the limited nature of the diffraction data (see Table 1) was restricting the refinement process. This was primarily because the exclusion of whole classes of reflexions from the data set prevented their interaction with the refined model.

To compensate for this, the reflexions for which data had not been collected, out to a 2θ limit of 50°, were given half the average intensity value of the 'less thans' threshold [*i.e.*, $1{\cdot}65\sigma(I)$] for each 2θ value. With the inclusion of these theoretical reflexions, the expanded data set consisted of 4129 intensities. The refinement process was continued for several possible structural models, the lowest R value being about 0·21 for all data and 0·18 excluding the 'less thans'.

Smaller maxima occurred in the difference maps, but the atomic parameters could not be determined accurately owing to the high correlation factors. The locations of the extra metal atoms were still uncertain, although it was apparent that these atoms occur in planes at $z=0$, $z\simeq 0{\cdot}25$, $z=\frac{1}{2}$ and $z\simeq 0{\cdot}75$. There was some evidence, however, based on the temperature factors (Hall & Rowland, 1973), that certain metal atoms were copper and others iron. These metal types were substituted for the copper–iron average atoms, and the R value decreased to about 0·17. Successive shifts in positional parameters and isotropic temperature factors resulted in an R value of about 0·15.

At this point the copper and iron atoms in the sphalerite-like sites had been tentatively identified, and 8 of the 12 extra metal atoms had been located in specific sites at $z\simeq 0{\cdot}25$ and $z\simeq 0{\cdot}75$. The locations of the other four extra metal atoms at $z=0$ and $z=\frac{1}{2}$ were still undetermined, and a survey was made of all the possible combinations. Thirty-six choices exist for locating two atoms at $z=0$ and at $z=\frac{1}{2}$, but these reduce to nine possibilities when origin shifts along a and b are considered.

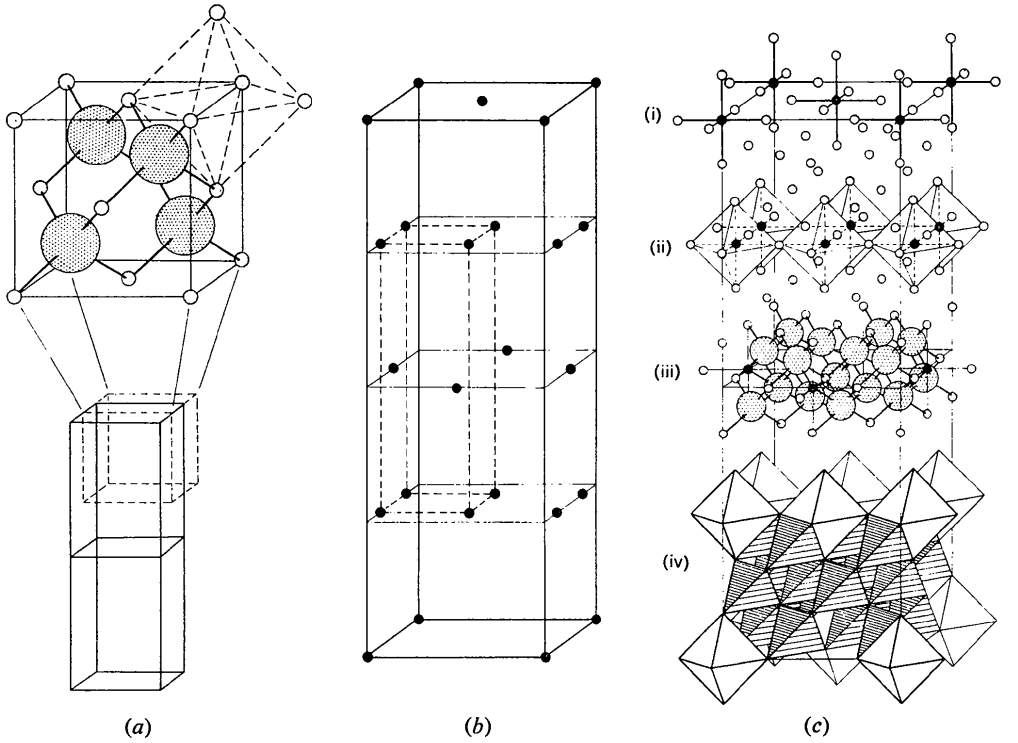

Fig. 2. (*a*) The sphalerite-like pseudo-cubic subcell containing tetrahedrally coordinated metal and sulphur atoms, with the octahedral arrangement of metal atoms about the interstitial sites indicated. Three pseudo-cubic subcells comprise the pseudo-tetragonal subcell. (*b*) Eight pseudo-tetragonal subcells, offset one-half cell in the **a** and **c** directions to permit correlation of the extra metal atoms, comprise the orthorhombic unit cell. (*c*) Atomic coordination in the orthorhombic unit cell: (i) octahedral coordination of extra metal atoms at 1(*a*) and 1(*e*) at $z=1$; (ii) octahedra about four extra metal atoms at 4(*u*) at $z\simeq 0{\cdot}75$; (iii) tetrahedral coordination of sulphur to metal atoms including extra at 1(*f*) and 1(*g*) at $z=\frac{1}{2}$; (iv) metal tetrahedra about sulphur atoms, and metal octahedra about extra metal atoms from $z=0$ to $z\simeq 0{\cdot}25$.

Table 2. *Atomic parameters*

The fractional atomic coordinates and site designations are based on the structural model with lowest R value (0·14) with space group $P222$ ($a \simeq 10{\cdot}7$, $b \simeq 10{\cdot}7$, $c \simeq 31{\cdot}6$ Å). The pseudo-tetragonal ($a \simeq b \simeq 5{\cdot}3$, $c \simeq 16{\cdot}0$ Å) site designations and average temperature factors ($\langle B \rangle = 8\pi^2 U$) are given for the same space group.

						Pseudo-tetragonal									Pseudo-tetragonal		
Atom	Type	Site	x	y	z	Site	U	$\langle B \rangle$	Atom	Type	Site	x	y	z	Site	U	$\langle B \rangle$
M1	Cu	2(*i*)	0·257	0	0	1(*d*)	0·020	1·58	S1	S	4(*u*)	0·119	0·127	0·042	4(*u*)	0·012	1·00
M2	Cu	2(*k*)	0·257	½	0				S2	S	4(*u*)	0·380	0·870	0·042			
M3	Cu	2(*j*)	0·250	0	½				S3	S	4(*u*)	0·123	0·628	0·042			
M4	Cu	2(*l*)	0·248	½	½				S4	S	4(*u*)	0·379	0·373	0·042			
M5	Fe	2(*m*)	0	0·255	0	1(*h*)	0·011	0·89	S5	S	4(*u*)	0·124	0·869	0·458			
M6	Fe	2(*o*)	½	0·259	0				S6	S	4(*u*)	0·375	0·132	0·458			
M7	Fe	2(*n*)	0	0·247	½				S7	S	4(*u*)	0·126	0·369	0·458			
M8	Fe	2(*p*)	½	0·252	½				S8	S	4(*u*)	0·376	0·630	0·458			
M9	Fe	4(*u*)	0·251	−0·001	0·165	2(*q*)	0·009	0·73	S9	S	4(*u*)	0·128	0·876	0·125	4(*u*)	0·015	1·16
M10	Fe	4(*u*)	0·248	0·488	0·166				S10	S	4(*u*)	0·371	0·124	0·125			
M11	Fe	4(*u*)	0·251	−0·002	0·335				S11	S	4(*u*)	0·129	0·376	0·125			
M12	Fe	4(*u*)	0·249	0·499	0·334				S12	S	4(*u*)	0·373	0·623	0·125			
M13	Cu	4(*u*)	−0·005	0·249	0·164	2(*t*)	0·024	1·87	S13	S	4(*u*)	0·128	0·122	0·375			
M14	Cu	4(*u*)	0·489	0·250	0·163				S14	S	4(*u*)	0·374	0·874	0·375			
M15	Cu	4(*u*)	0·002	0·249	0·336				S15	S	4(*u*)	0·128	0·624	0·375			
M16	Cu	4(*u*)	0·498	0·250	0·336				S16	S	4(*u*)	0·372	0·377	0·375			
M17	Fe	2(*q*)	0	0	0·086	2(*r*)	0·011	0·87	S17	S	4(*u*)	0·126	0·122	0·208	4(*u*)	0·011	0·87
M18	Fe	2(*r*)	½	0	0·086				S18	S	4(*u*)	0·378	0·876	0·208			
M19	Fe	2(*s*)	0	½	0·086				S19	S	4(*u*)	0·123	0·623	0·208			
M20	Fe	2(*t*)	½	½	0·086				S20	S	4(*u*)	0·373	0·380	0·208			
M21	Fe	2(*q*)	0	0	0·414				S21	S	4(*u*)	0·126	0·875	0·292			
M22	Fe	2(*r*)	½	0	0·414				S22	S	4(*u*)	0·376	0·124	0·292			
M23	Fe	2(*s*)	0	½	0·414				S23	S	4(*u*)	0·126	0·377	0·292			
M24	Fe	2(*t*)	½	½	0·414				S24	S	4(*u*)	0·374	0·625	0·292			
M25	Cu	4(*u*)	0·252	0·245	0·086	2(*s*)	0·021	1·68									
M26	Cu	4(*u*)	0·246	0·748	0·086												
M27	Cu	4(*u*)	0·249	0·251	0·414												
M28	Cu	4(*u*)	0·251	0·751	0·415												
M29	Cu	2(*q*)	0	0	0·250	1(*b*)	0·019	1·52	M35	Fe	4(*u*)	0·251	−0·001	0·250	1(*a*)	0·010	0·81
M30	Cu	2(*r*)	½	0	0·250				M36	Fe	4(*u*)	0·249	0·500	0·250			
M31	Cu	2(*s*)	0	½	0·250				M37	Fe	1(*a*)	0	0	0	1(*f*)	0·016	1·24
M32	Cu	2(*t*)	½	½	0·250				M38	Fe	1(*e*)	½	½	0		P.P. = ½	
M33	Fe	4(*u*)	0·251	0·249	0·250	1(*c*)	0·009	0·71	M39	Fe	1(*f*)	½	0	½			
M34	Fe	4(*u*)	0·250	0·750	0·250				M40	Fe	1(*g*)	0	½	½			

For each of these nine models of haycockite, successive structure-factor calculations and electron-density difference maps were obtained. The indicated parameter shifts were made before each new calculation, and work on each model was discontinued when the R value showed no change. For two of the nine models R increased slightly, and stayed at about 0·15; for five models R decreased only slightly below 0·15; for the other two models, R decreased to 0·14.

The systematic-absence conditions did not permit the determination of the space group with certainty, $P222$, $P222_1$, $P2_12_12$ and $P2_12_12_1$ all being possible. Because of the flexibility in locating the extra metal atoms $P222$ was selected, and for this space group the two models that refined to the lowest R value, 0·14, contain interstitial metal atoms at 1(*a*) (0,0,0), 1(*e*) $(\frac{1}{2},\frac{1}{2},0)$, 1(*f*) $(\frac{1}{2},0,\frac{1}{2})$, 1(*g*) $(0,\frac{1}{2},\frac{1}{2})$ and at 1(*a*) (0,0,0), 1(*b*) $(\frac{1}{2},0,0)$, 1(*f*) $(\frac{1}{2},0,\frac{1}{2})$, 1(*h*) $(\frac{1}{2},\frac{1}{2},\frac{1}{2})$, respectively, in addition to two 4(*u*) (x,y,z) sites. The former refined to a slightly lower R value, and can also be described in space groups $P2_12_12_1$ and $P2_12_12$. This model is shown in Fig. 2, and the atomic coordinates are listed in Table 2. For both models the location of the additional interstitial metals and the proposed ordering of the copper and iron atoms satisfy the expected structural aspects, *viz.* subcells and relative cell size. The limited extent and accuracy of the diffraction data did not warrant further analysis. Structure factors are listed in Table 3.

Table 3. *Structure factors listed in blocks of constant k l in columns of h, F_m and F_c*

An asterisk denotes reflexions with $I_{net} > 1{\cdot}65\ \sigma(I)$.

Description of the structure

This study shows that the structure of haycockite is based on a sphalerite-like arrangement of metal and sulphur atoms, as are the structures of other chalcopyrite-like minerals. This confirms that all minerals with compositions in the central portion of the Cu–Fe–S system exist at some temperature as a sphalerite-like ABC arrangement of close-packed layers of sulphur atoms that are tetrahedrally coordinated to the copper and iron atoms.

In haycockite, three sphalerite-like pseudo-cubic cells, with $a \simeq 5{\cdot}3$ Å, are combined along one axis to give a pseudo-tetragonal cell with $a \simeq 5{\cdot}3$, $c \simeq 16$ Å, and eight of these pseudo-tetragonal cells, two along each axis, comprise the true orthorhombic unit cell. The tetrahedrally coordinated metal and sulphur atoms account for 48 formula units of $CuFeS_2$. The 12 additional iron atoms required to give the unit-cell composition of $Cu_{48}Fe_{60}S_{96}$ are distributed in interstices of the sphalerite-like structure. Although the proposed distribution for the interstitial metal atoms in the orthorhombic unit cell is not unequivocal, it does comply with all the explicit crystal and diffraction requirements.

The location of extra metal atoms in adjacent interstitial sites along the a and b axes, at levels of $z \simeq 0{\cdot}25$ and $z \simeq 0{\cdot}75$, explains the expansion of the sphalerite-like pseudo-cubic subcell ($a \simeq 5{\cdot}3$ Å) along these axes ($2 \times 5{\cdot}35$ and $2 \times 5{\cdot}37$ Å) relative to the c axis ($6 \times 5{\cdot}27$ Å). Along the c axis the extra metal atoms are not located in adjacent interstitial sites, and cell expansion does not occur in this direction. The average metal–metal distance when interstitial metals are adjacent (at $z \simeq 0{\cdot}25$ and $z \simeq 0{\cdot}75$) is 2·68 (2) Å along the a and b axes, and 2·68 (1) Å along the c axis. For isolated interstitial atoms (at $z=0$ and $z=\frac{1}{2}$), these distances are 2·67 (8) Å along the a axis, 2·69 (10) Å along the b axis, and 2·72 (1) Å along the c axis. The average sulphur–metal distances are S–Cu = 2·32 (11), S–Fe = 2·30 (14), and S–M(extra) = 2·31 (5) Å.

Evidence for identifying metal atoms as either copper or iron was based in large part on the value of the isotropic temperature factor, which is known from other chalcopyrite-like minerals to be larger for copper than for iron atoms (Hall & Stewart, 1973; Szymanski, 1974). In general, the values of the average metal–sulphur distances are consistent with the metals identified on this basis. The temperature factors given in Table 2 were determined in terms of the equivalent pseudo-tetragonal sites, and are consistently higher for copper atoms than for iron atoms. All the extra metal atoms are considered to be iron atoms. The assignment of metal types for the basic sphalerite-like

arrangement of atoms conforms to a pattern related to the locations of the extra metal atoms. Two copper atoms and four iron atoms surround 16 interstitial sites, and these include the locations of the 12 extra metal atoms. Two iron atoms and four copper atoms surround 16 other interstitial sites at the same level along the **c** direction. The remaining 64 interstitial sites are surrounded by three copper and three iron atoms, and these do not contain extra metal atoms.

The copper and iron atoms in planes normal to the **c** direction are ordered alternately, as in chalcopyrite. The repeat distance of these metal planes is four intervals (*ca.* 10·5 Å) in chalcopyrite, and six intervals (*ca.* 15·8 Å) in haycockite. In haycockite there are two repeats for the entire unit cell (*ca.* 31·6 Å). In addition to the repeat distance, the metal ordering is mirrored across these planes at $z=0$, $z\simeq 0{\cdot}25$, $z=\frac{1}{2}$, $z\simeq 0{\cdot}75$, the levels at which the extra metal atoms are located. The extra metal sites all have adjacent copper atoms in the **a** direction and adjacent iron atoms in the **b** direction, and an examination of the arrangement of metal atoms in the sphalerite-like structure shows two different patterns of ordering in planes normal to the **a** and **b** directions. These atomic arrangements are consistent with haycockite being orthorhombic, rather than tetragonal, even though the difference in the lengths of the *a* and *b* axes is only about 0·3%.

We are indebted to Dr L. J. Cabri for supplying the haycockite crystals, to Mr J. M. Stewart for his assistance in the preliminary X-ray photographic survey, to Mr D. Lister for the preparation of the diagrams, and to participants of the Mineral Research Program for their valuable discussions.

References

BUSING, W. R. (1970). *Crystallographic Computing*, edited by F. R. AHMED, pp. 319–330. Copenhagen: Munksgaard.

CABRI, L. J. (1973). *Econ. Geol.* **68**, 433–454.

CABRI, L. J. & HALL, S. R. (1972). *Amer. Min.* **57**, 689–708.

CROMER, D. T. & MANN, J. B. (1968). *Acta Cryst.* A**24**, 321–324.

GABE, E. J. & O'BYRNE, T. (1970). Amer. Cryst. Assoc. Summer Meeting, Abstracts. Paper A4.

HALL, S. R. & GABE, E. J. (1972). *Amer. Min.* **57**, 368–380.

HALL, S. R. & ROWLAND, J. F. (1973). *Acta Cryst.* B**29**, 2365–2372.

HALL, S. R. & STEWART, J. M. (1973). *Acta Cryst.* B**29**, 579–586.

STEWART, J. M., KRUGER, G. J., AMMON, H. L., DICKINSON, C. & HALL, S. R. (1972). Univ. Maryland Comput. Sci. Tech. Rep. TR-192.

SZYMANSKI, J. T. (1974). *Z. Kristallogr.* **140**, 218–239.

TOMIIE, Y. & STAM, C. H. (1958). *Acta Cryst.* **11**, 126–127.